Journal of Solid Mechanics Vol. 11, No. 2 (2019) pp. 388-408
DOI: 10.22034/JSM.2019.665161

Strain Hardening Analysis for *M-P* Interaction in Metallic Beam of *T*-Section

M. Hosseini [1,*], H. Hatami [2]

[1]*Department of Civil Engineering, Faculty of Engineering, Lorestan University, Iran*
[2]*Department of Mechanical Engineering , Faculty of Engineering, Lorestan University, Iran*

Received 8 March 2019; accepted 8 May 2019

ABSTRACT

This paper derives kinematic admissible bending moment – axial force (*M-P*) interaction relations for mild steel by considering strain hardening idealisations. Two models for strain hardening – Linear and parabolic have been considered, the parabolic model being closer to the experiments. The interaction relations can predict strains, which is not possible in a rigid, perfectly plastic idealization. The relations are obtained for all possible cases pertaining to the locations of neutral axis. One commercial rolled steel *T*-section has been considered for studying the characteristics of interaction curves for different models. On the basis of these interaction curves, most significant cases for the position of neutral axis which are enough for the establishment of interaction relations have been suggested. The influence of strain hardening in the interaction study has been highlighted. The strains and hence the strain rates due to bending and an axial force can be separated only for the linear-elastic case because the principle of superposition is not valid for the nonlinear case. The difference between the interaction curves for linear and parabolic hardening for the particular material is small.

Keywords : Axial force; Bending moment; *T*–Section; *M-P* interaction; Strain hardening.

1 INTRODUCTION

STUDY of structural failure under impact loading is of importance for the safety and hazard assessment of structures. Simple structural elements like beams, plates and shells fail in different modes under dynamic loading. The beams being relatively critical elements have attracted more attention of scientists and engineers. The membrane force plays an important role in the dynamic response of a beam when the transverse deformations are sufficiently large, thus requiring axial force – bending moment interaction relations up to failure. Standard static methods of analysis with dynamic magnification factors, for example, are not adequate in many dynamic plastic structural problems. Structural designers are often required to estimate the failure load of structural members for which they employ numerical techniques, such as the finite element method, but the analysis up to failure with large

*Corresponding author.
E-mail address: hoseini.m@lu.ac.ir (M. Hosseini).

displacements and strains is usually difficult. An early experimental study on the dynamic, inelastic failure of beams was reported by Menkes and Opat [1] who investigated the dynamic plastic response and failure of fully clamped metal beams which were subjected to uniformly distributed velocities over the entire span. They observed that the beams responded in a ductile manner and acquired permanently deformed profiles when subjected to velocities less than a certain value. However, when the impulsive velocities were equal to this critical value, then the beams failed owing to tearing of the beam material at the supports. As the impulsive velocities were further increased beyond this critical value, failure occurred, and the plastic deformation of the beams become more localized near the supports until another critical velocity, which was associated with a transverse shear failure at the supports, was reached. The experimental results of Menkes and Opat [1] were later analysed by Jones [2] using a simple rigid-plastic method. A systematic study on the deformation and failure of fully clamped ductile beams struck by a mass has been conducted by Liu and Jones [3,4]. Two modes of failure – Tensile tearing and shear failure modes – have been observed in experiments depending on the uniaxial rupture strain of the materials, the location of impact point and support conditions. The experiments on Aluminium beams showed that the geometry changes for finite deflection play an important role in the dynamic response and higher modal dynamic plastic response of the beams is more efficient in absorbing kinetic energy than single modal response [5]. In a rigid-plastic structure, Shen and Jones [6] assumed that the rupture occurs when the absorption of plastic work per unit volume reached a critical value. To calculate the actual plastic work in beams, a hinge length was estimated from experimental data obtained by Menkes and Opat [1] on impulsively loaded aluminium beams. Continuum damage mechanics has been used recently by Alves and Jones [7] for predicting the static and dynamic failure of beams, but the method requires the values for several parameters, some of which are difficult to obtain. The theoretical anomalous dynamic response of beams [8,9] and plates [10] for a short pulse loading causing small deflections has been studied by elastic-plastic material model. Another simpler and more attractive option for some problems is to carry out a rigid perfectly plastic analysis that have been used by several authors e.g. Lellep and Torn [11], Ma et al.[12] and Ghaderi et al. [13]. The accuracy of which has been compared with the predictions of an elastic-plastic material [14-18] However, a rigid, perfectly plastic analysis does not predict strains so that it is difficult to study failure unless some assumptions are made to overcome this difficulty.

In the present paper, kinematic admissible interaction curves for the simultaneous action of bending moment and an axial force on a *T*-section have been developed for strain-hardening material idealisations. Two models for strain hardening – Linear and parabolic have been considered. The interaction curves developed for *T*-section may be easily degenerated to rectangular section. The procedure requires only the results from a standard uniaxial tensile test on the material. The strains and hence the strain rates due to bending and an axial force can be separated only for the linear-elastic case because the principle of superposition is not valid for the nonlinear case. The difference between the interaction curves for linear and parabolic hardening for the particular material is small.

2 STRESS-STRAIN DIAGRAM

Direct tensile test results by Alves and Jones [19] for a mild steel specimen 't036' as shown in Fig. 1 are taken as a reference for the modelling of stress-strain diagram, which is thus idealised as linear for elastic strains followed by flat yielding zone without strain hardening. Therefore, the strain hardening has been modelled by linear and parabolic models (Fig. 1). Thus, there are three zones in the idealised diagram: elastic zone from $k = 0$ to $k = 1$; yield zone without any strain-hardening from $k = 1$ to $k = k_1$; and the strain-hardening zone from $k = k_1$ to $k = k_2$, where, $k\,\varepsilon_y$ is the strain. The stress in the strain-hardening range, σ_d, at any strain, $\varepsilon = k\,\varepsilon_y$ $\left(k_1 \le k \le k_2\right)$, can be obtained from the following relations:

$$\sigma_d = \sigma_{yd} + \left(\sigma_{ud} - \sigma_{yd}\right) m \quad \text{for Linear-Hardening} \tag{1}$$

$$\sigma_d = \sigma_{yd} + \left(\sigma_{ud} - \sigma_{yd}\right)\left(2m - m^2\right) \quad \text{for Parabolic-Hardening} \tag{2}$$

where,

$$m = \left(\frac{\varepsilon - \varepsilon_h}{\varepsilon_u - \varepsilon_h} \right) = \left(\frac{k - k_1}{k_2 - k_1} \right) \tag{3}$$

where, ε_h ($= k_1 \varepsilon_y$) is strain corresponding to the initiation of strain hardening and ε_u ($= k_2 \varepsilon_y$) is the ultimate strain, σ_{yd} and σ_{ud} are the yield and ultimate dynamic stresses respectively. The suffix *d* in the above expressions has been used to indicate dynamic values. The stress-strain curve can be used for high strength steel by substituting $k_1 = 1$ and many other materials can be easily represented by these equations for different values of the parameters.

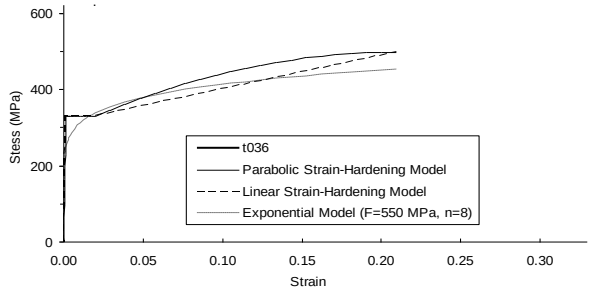

Fig.1
Experimental stress-strain curve and different models of mild steel.

3 BENDING MOMENT-AXIAL FORCE (*M-P*) INTERACTION

Considering a *T*-section of beam with width of flange, *B*, thickness of flange, *h*, overall depth, *H*, and the thickness of web, *b*, for studying the interaction of a bending moment, *M*, and an axial force, *P* (Fig. 2). The geometry of the section is defined by the following non-dimensional parameters:

$$\left.\begin{aligned} \alpha &= h / H \\ \beta &= \left(B - b\right)/B \\ \gamma &= b / B \\ \gamma_1 &= \alpha\beta\left(1-\alpha\right) \end{aligned}\right\} \tag{4}$$

The *T*-section converts to the rectangular section when, $\alpha = 0$ or 1, $\beta = 0$, $\gamma = 1$, $\gamma_1 = 0$. The bending moment is assumed to cause compression at the top face. The axial force considered in the present analysis is tensile and the same relations can be used for a compressive axial force because the material behaviour in compression has been assumed to be the same as in tension. The interaction curves for different states of stresses have been obtained in the subsequent subsections.

The extreme fibre strain in tension (i.e. at the bottom fibre) is taken as $k\,\varepsilon_y$ and the strain at the interface of web with top flange is $k_t \varepsilon_y$. The extreme fibre strain at the top fibre is taken as $k'\varepsilon_y$ which is compressive when the neutral axis is inside the section, whereas, it is tensile when the neutral axis is outside the section. The value of k' and k_t when the neutral axis lies inside the section (Fig. 3) are given by

$$k' = k\,\frac{r}{1-r} \tag{5}$$

and

$$k_t = k\,\frac{r-\alpha}{1-r} \tag{6}$$

where, $r = H_1/H$; H_1 = distance of the neutral axis from the extreme compression fibre. Whereas, when the neutral axis lies outside the section (Fig. 3), the value of k' and k_t are given by:

$$k' = k\,\frac{r}{1+r} \tag{7}$$

and

$$k_t = k\,\frac{r+\alpha}{1+r} \tag{8}$$

There are well-established interaction curves for elastic and a rigid, perfectly plastic section having a rectangular cross-section [5] (see Jones, 1997), whereas for *T*-section these are derived in this Section.

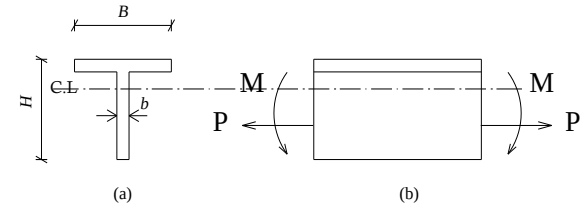

Fig.2
(a) Section of beam, (b) An element subjected to external pull and bending moment.

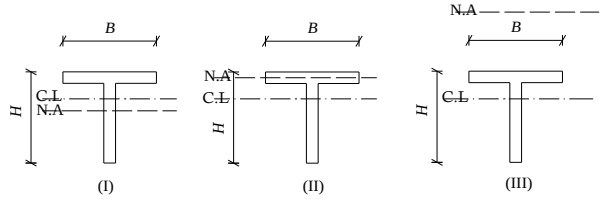

Fig.3
Positions of neutral axis: (I) Neutral axis in web, (II) Neutral axis in flanges and (III) Neutral axis outside the section.

3.1 Elastic

Case I

Neutral axis lies in the web i.e. $0 \le k' \le 1$ (Fig. 4(a)).

The *M-P* interaction relation obtained for this case is:

$$\bar{M} = \frac{2\alpha_1}{1-r}\left[\gamma(1-r)^3 + \beta(\alpha-r)^3 + r^3 - \frac{3}{2}\beta_1\bar{P}(\psi-2r)(1-r)\right] \tag{9}$$

where,

$$r = \frac{\alpha^2\beta + \gamma - 2\beta_1\bar{P}}{2\left(\alpha\beta + \gamma - \beta_1\bar{P}\right)} \tag{10a}$$

$$\alpha_1 = M_{1yd}/M_{yd} \tag{10b}$$

$$\beta_1 = P_{yd}/P_{1yd} \tag{10c}$$

$$P_{1yd} = \sigma_{yd}BH \tag{10d}$$

$$M_{1yd} = \sigma_{yd} BH^2 / 6 \tag{10e}$$

$$\bar{P} = P / P_{yd} \tag{10f}$$

$$\psi = \frac{\alpha^2 + \gamma\left(1-\alpha^2\right)}{\alpha + \gamma\left(1-\alpha\right)} \tag{10g}$$

$$\bar{M} = \frac{M}{M_{yd}} \tag{10h}$$

$$P_{yd} = \sigma_{yd}\left[BH - \left(B-b\right)\left(H-h\right)\right] \tag{10i}$$

$$M_{yd} = \frac{\sigma_{yd} BH^2}{6\psi}\left\{\alpha^3\beta\left[1+3\left(\frac{\psi}{\alpha}-1\right)^2\right] + \gamma\left[1+3\left(1-\psi\right)^2\right]\right\} \tag{10j}$$

Eq. (9) converts to the rectangular section for $\alpha = 0$ or 1, $\beta = 0$, $\gamma = 1$, $\alpha_1 = 1$ and $\beta_1 = 1$ thus giving

$$\psi = 1 \tag{11a}$$

$$M_{yd} = \frac{BH^2}{6} \tag{11b}$$

$$\overline{M} + \overline{P} = 1 \tag{11c}$$

Case II

Neutral axis lies in the flange i.e. $0 \le k' \le 1$ (Fig. 4(b)).

The *M-P* interaction relation obtained for this case is:

$$\bar{M} = \frac{2\alpha_1}{1-r}\left[\gamma\left(1-r\right)^3 + \beta\left(\alpha-r\right)^3 + r^3 - \frac{3}{2}\beta_1\bar{P}\left(\psi-2r\right)\left(1-r\right)\right] \tag{12}$$

The non-dimensional distance of the neutral axis, *r*, required for determining the value of k' from Eq. (5) may be obtained from the equation:

$$r = \frac{\alpha^2\beta + \gamma - 2\beta_1\bar{P}}{2\left(\alpha\beta + \gamma - \beta_1\bar{P}\right)} \tag{13}$$

Case III

Neutral axis is outside the section i.e. $0 \le k' \le 1$ (Fig. 4(c)).

The *M-P* interaction relation obtained for this case is:

$$\bar{M} = \frac{2\alpha_1}{1+r}\left[\gamma\left(1+r\right)^3 + \beta\left(\alpha+r\right)^3 - r^3 - \frac{3}{2}\beta_1\bar{P}\left(\psi+2r\right)\left(1+r\right)\right] \tag{14}$$

The non-dimensional distance of the neutral axis, *r*, required for determining the value of k' from Eq. (7) may be obtained from the equation:

$$r = -\frac{\alpha^2\beta + \gamma - 2\beta_1\bar{P}}{2\left(\alpha\beta + \gamma - \beta_1\bar{P}\right)} \tag{15}$$

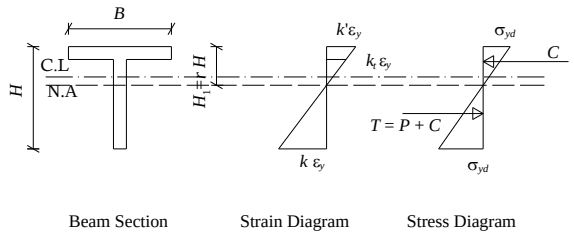

(a) Neutral axis lies in the web i.e. $0 \le k' \le 1$.

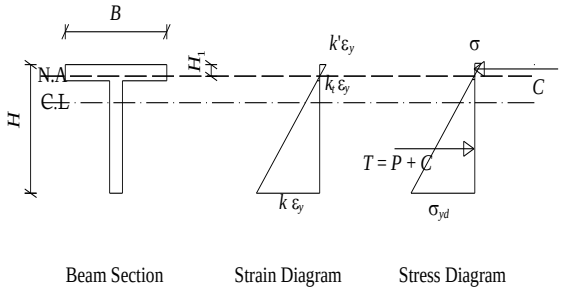

(b) Neutral axis lies in the flange i.e. $0 \le k' \le 1$.

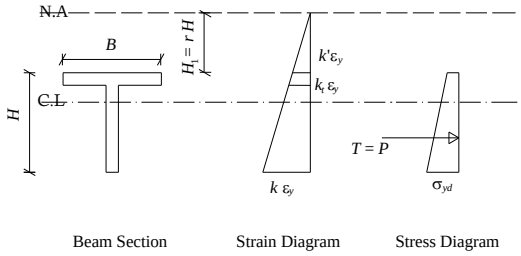

(c) Neutral axis is outside the section i.e. $0 \le k' \le 1$.

Fig.4
Stress and strain variation in the section of a beam for different positions of neutral axis in the elastic model.

3.2 Plastic

For Rigid Perfectly Plastic case, there are two cases – one in which the neutral axis lies in the web and the other wherein neutral axis lies in the flange. These two cases are discussed in subsequent sub-sections.

Case I
Neutral axis lies in the web i.e. $1 \le k' \le k_1$ (Fig. 5(a)).

The *M-P* interaction relation obtained for this case is:

$$\bar{M} = 3\alpha_1\left[\gamma(1-r)^2 - \beta(r-\alpha)^2 + r^2 - \beta_1\bar{P}(\psi - 2r)\right] \tag{16}$$

$$r = -\frac{\alpha\beta - \gamma + \beta_1\bar{P}}{2\gamma} \tag{17}$$

The above equation converts to the rectangular section for $\alpha = 0$ or 1, $\beta = 0$, $\gamma = 1$, $\alpha_1 = 1$ and $\beta_1 = 1$ thus giving

$$\frac{2}{3}\overline{M} + \overline{P}^2 = 1 \tag{18}$$

Case II
Neutral axis lies inside the flange i.e. $1 \le k' \le k_1$ (Fig. 5(b)).

The *M-P* interaction relation obtained for this case is:

$$\bar{M} = 3\alpha_1\left[\gamma(1-r)^2 + \beta(\alpha-r)^2 + r^2 - \beta_1\bar{P}(\psi-2r)\right] \tag{19}$$

$$r = \frac{\alpha\beta+\gamma-\beta_1\bar{P}}{2} \tag{20}$$

The cross-section can only become fully plastic when the extreme fibre strain is infinite, which practically, is not possible. The advantage of Eqs. (16) and (19) lies in their simplicity but the main disadvantage is that it cannot predict strains. To overcome this difficulty the strain hardening case is considered in the next subsection, which almost reduces to the rigid, perfectly plastic model for a large yield zone.

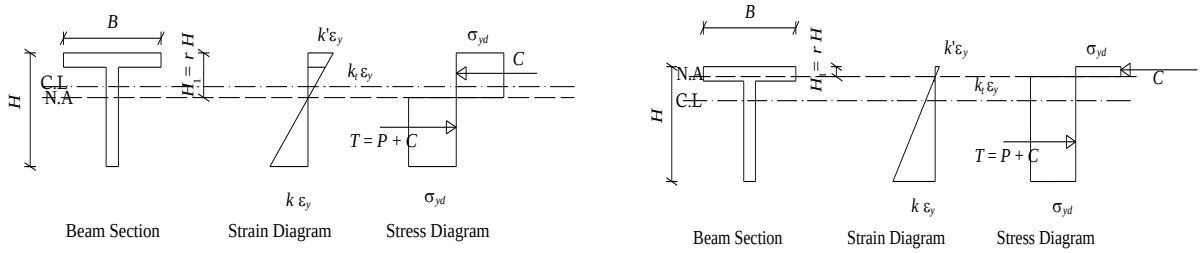

(a) Neutral axis lies in the web i.e. $1 \le k' \le k_1$.

(b) Neutral axis lies inside the flange i.e. $1 \le k' \le k_1$.

Fig.5
Stress and strain variation in the section of a beam for different positions of neutral axis in the rigid perfectly plastic model.

3.3 Strain-hardening models

For linear as well as parabolic strain hardening, there are eleven cases depending upon the position of the neutral axis, six cases for the neutral axis inside and five cases for neutral axis outside the section as shown in Figs. 6 and 7. The extreme fibre strain at the top is compressive when the neutral axis lies inside the section, whereas, it is tensile when the neutral axis is outside the section. The relations obtained for these cases for the two types of hardening are given in the subsequent sections. The proof of Case I for parabolic-hardening, is given in Appendix A. The remaining expressions can be derived in a similar way.

3.3.1 Linear-hardening

For the linear hardening model, the ten cases, which depend upon the position of the neutral axis, are presented below:

Case I
Neutral axis lies in the web i.e. $k_1 \le k' \le k_2$ and $k_1 \le k_t \le k_2$ (Fig. 6(a)).

The *M-P* interaction relation obtained for this case is:

$$\bar{M} = 3\alpha_1\left[\begin{array}{l}\alpha\beta(r-2\alpha) - \gamma\left(\frac{r}{k'}\right)^2\left(\frac{2}{3}-k^2\right) - (\psi-2r)\beta_1\bar{P} \\ +\gamma r^2 + \frac{2S_L}{3}\left(\frac{r}{k'}\right)^2\left[\gamma a_1^2 f_L - \beta b_1^2 g_L + c_1^2 h_L\right]\end{array}\right] \tag{21}$$

The non-dimensional distance of the neutral axis, *r*, required in the above equation and also for determining the value of k' from Eq. (5) may be obtained from the quadratic equation:

The extreme fibre strain at the top fibre is taken as $k'\varepsilon_y$ which is compressive when the neutral axis is inside the section, whereas, it is tensile when the neutral axis is outside the section. The value of k' and k_t when the neutral axis lies inside the section (Fig. 3) are given by $k' = k\,\frac{r}{1-r}$ Whereas, when the neutral axis lies outside the section (Fig. 3), the value of k' and k_t are given by: $k' = k\,\frac{r}{1+r}$ and $k_t = k\,\frac{r+a}{1+r}$.

$$\gamma\left[2+\frac{S_L}{k}\left(a_1^2-d_1^2\right)\right]r^2-\left[3\gamma+2\frac{S_L}{k}\left\{\gamma a_1^2+\beta d_1 e_1-k_1 d_1\right\}-\alpha\beta-\beta_1\bar{P}\right]r+\left[\gamma+\frac{S_L}{k}\left\{\gamma a_1^2-k_1^2+\beta e_1^2\right\}-\alpha\beta-\beta_1\bar{P}\right]=0 \tag{22}$$

where

$$S_L=\frac{1}{2(k_2-k_1)}\left(\frac{\sigma_{ud}}{\sigma_{yd}}-1\right) \tag{23a}$$

$$a_1=k-k_1 \tag{23b}$$

$$b_1=k_t-k_1 \tag{23c}$$

$$c_1=k'-k_1 \tag{23d}$$

$$d_1=k+k_1 \tag{23e}$$

$$e_1=\alpha k+k_1 \tag{23f}$$

$$f_L=2k+k_1 \tag{23g}$$

$$g_L=2k_t+k_1 \tag{23h}$$

$$h_L=2k'+k_1 \tag{23i}$$

Case II

Neutral axis lies in the web i.e. $k_1 \le k' \le k_2$ and $1 \le k_t \le k_1$ (Fig. 6(b)).

The *M-P* interaction relation obtained for this case is:

$$\bar{M}=3\alpha_1\left[\begin{array}{l}\alpha\beta(2r-\alpha)-\gamma\left(\frac{r}{k'}\right)^2\left(\frac{2}{3}-k^2\right)-(\psi-2r)\beta_1\bar{P}\\ +\gamma r^2+\frac{2S_L}{3}\left(\frac{r}{k'}\right)^2\left[\gamma a_1^2 f_L+c_1^2 h_L\right]\end{array}\right] \tag{24}$$

The non-dimensional distance of the neutral axis, *r*, required in the above equation and also for determining the value of k' from Eq. (5) may be obtained from the quadratic equation:

$$\left[2\gamma+\frac{S_L}{k}\left(\gamma a_1^2-d_1^2\right)\right]r^2-\left[3\gamma-\alpha\beta+2\frac{S_L}{k}\left\{\gamma a_1^2-k_1 d_1\right\}-\beta_1\bar{P}\right]r+\left[\gamma-\alpha\beta+\frac{S_L}{k}\left\{\gamma a_1^2-k_1^2\right\}-\beta_1\bar{P}\right]=0 \tag{25}$$

Case III

Neutral axis lies in the web i.e. $1 \le k' \le k_1$ and $0 \le k_t \le 1$ (Fig. 6(c)).

The *M-P* interaction relation obtained for this case is:

$$\bar{M} = 3\alpha_1 \left[\gamma r^2 + \alpha\beta(2r-\alpha) - \gamma\left(\frac{r}{k'}\right)^2 \left(\frac{2}{3} - k^2\right) + \frac{2S_L}{3}\left(\frac{r}{k'}\right)^2 \gamma a_1^2 f_L - (\psi - 2r)\beta_1 \bar{P} \right] \tag{26}$$

The non-dimensional distance of the neutral axis, *r*, required in the above equation and also for determining the value of k' from Eq. (5) may be obtained from the quadratic equation:

$$\gamma\left(2 + \frac{S_L}{k} a_1^2\right) r - \left[\gamma - \alpha\beta + \frac{S_L}{k}\gamma a_1^2 - \beta_1 \bar{P}\right] = 0 \tag{27}$$

Case IV

Neutral axis lies in the web i.e. $1 \le k' \le k_1$ and $0 \le k_t \le 1$ (Fig. 6(d)).

The *M-P* interaction relation obtained for this case is:

$$\bar{M} = 3\alpha_1 \left[\begin{array}{l} r^2 - \left(\frac{r}{k'}\right)^2 \left\{ \frac{1}{3}(1+\gamma) - \gamma k^2 + \frac{2}{3}\beta k_t^3 \right\} \\ + \frac{2S_L}{3}\left(\frac{r}{k'}\right)^2 \gamma a_1^2 f_L - (\psi - 2r)\beta_1 \bar{P} \end{array} \right] \tag{28}$$

The non-dimensional distance of the neutral axis, *r*, required in the above equation and also for determining the value of k' from Eq. (5) may be obtained from the quadratic equation:

$$\left[1 + \gamma + \frac{\beta}{2k} + \frac{\beta k}{2} + \frac{S_L}{k}\gamma a_1^2\right] r^2 - \left[1 + 2\gamma + \alpha\beta k + \frac{\beta}{k} + 2\frac{S_L}{k}\gamma a_1^2 - \beta_1 \bar{P}\right] r + \left[\gamma + \frac{1}{2}\alpha^2 \beta k + \frac{\beta}{2k} + \frac{S_L}{k}\gamma a_1^2 - \beta_1 \bar{P}\right] = 0 \tag{29}$$

Case V

Neutral axis lies in the flange i.e. $0 \le k' \le 1$ and $0 \le k_t \le 1$ (Fig. 6(e)).

The *M-P* interaction relation obtained for this case is:

$$\bar{M} = 3\alpha_1 \left[\begin{array}{l} r^2 - \frac{1}{3}\left(\frac{r}{k'}\right)^2 \left(1 + 2\gamma - \gamma k^2 - 2\beta k_t^3\right) \\ + \frac{2S_L}{3}\left(\frac{r}{k'}\right)^2 \gamma a_1^2 f_L - (\psi - 2r)\beta_1 \bar{P} \end{array} \right] \tag{30}$$

The non-dimensional distance of the neutral axis, *r*, required in the above equation and also for determining the value of k' from Eq. (5) may be obtained from the quadratic equation:

$$\left[1 + \gamma + \frac{\beta}{2k} + \frac{\beta k}{2} + \frac{S_L}{k}\gamma a_1^2\right] r^2 - \left[1 + 2\gamma + \alpha\beta k + \frac{\beta}{k} + \frac{2S_L}{k}\gamma a_1^2 - \beta_1 \bar{P}\right] r + \left[\gamma + \frac{\beta}{2k} + \frac{\alpha^2 \beta k}{2} + \frac{S_L}{k}\gamma a_1^2 - \beta_1 \bar{P}\right] = 0 \tag{31}$$

Case VI

Neutral axis lies in the flange i.e. $0 \le k' \le 1$ and $0 \le k_t \le 1$ (Fig. 6(f)).

The *M-P* interaction relation obtained for this case is:

$$\bar{M} = 3\alpha_1 \begin{bmatrix} \frac{1}{3}\left(\frac{r}{k'}\right)^2 \left\{\gamma k^2 - \gamma + 2\left(k'\right)^3 + 2\beta k_t^3\right\} \\ + \frac{2S_L}{3}\left(\frac{r}{k'}\right)^2 \gamma a_1^2 f_L - \left(\psi - 2r\right)\beta_1 \bar{P} \end{bmatrix} \tag{32}$$

The non-dimensional distance of the neutral axis, *r*, required in the above equation and also for determining the value of k' from Eq. (5) may be obtained from the quadratic equation:

$$\left[\gamma\left(1-\frac{1}{2k}\right) - \frac{k}{2} + \frac{\beta k}{2} + \frac{S_L}{k}\gamma a_1^2\right] r^2 - \left[\alpha\beta k + \gamma\left(2-\frac{1}{k}\right) + \frac{2S_L}{k}\gamma a_1^2 - \beta_1 \bar{P}\right] r + \left[\frac{\alpha^2 \beta k}{2} + \gamma\left(1-\frac{1}{2k}\right) + \frac{S_L}{k}\gamma a_1^2 - \beta_1 \bar{P}\right] = 0 \tag{33}$$

Case VII

Neutral axis lies outside the section i.e. $0 \le k' \le 1$ and $0 \le k_t \le 1$ (Fig. 7(a)).

The *M-P* interaction relation obtained for this case is:

$$\bar{M} = 3\alpha_1 \begin{bmatrix} \gamma\left(1+2r\right) - \frac{1}{3}\left(\frac{r}{k'}\right)^2 \gamma g_1^2 h_1 - \frac{\alpha^2 \beta k}{3}\frac{\alpha + 3r}{1+r} \\ + \alpha\beta k_t \left(\alpha + 2r\right) + \frac{2S_L}{3}\left(\frac{r}{k'}\right)^2 \gamma a_1^2 f_L - \left(\psi + 2r\right)\beta_1 \bar{P} \end{bmatrix} \tag{34}$$

where,

$$g_1 = 1 - k' \tag{35a}$$

$$h_1 = 1 + 2k' \tag{35b}$$

The non-dimensional distance of the neutral axis, *r*, required in the above equation and also for determining the value of k' from Eq. (7) may be obtained from the quadratic equation:

$$\left[-\gamma\frac{\left(1-k\right)^2}{2k} + \frac{S_L}{k}\gamma a_1^2\right] r^2 + \left[\alpha\beta k + 2\gamma - \frac{\gamma}{k} - 2\frac{S_L}{k}\gamma a_1^2 - \beta_1 \bar{P}\right] r + \left[\frac{\alpha^2 \beta k}{2} + \gamma\left(1-\frac{1}{2k}\right) + \frac{S_L}{k}\gamma a_1^2 - \beta_1 \bar{P}\right] = 0 \tag{36}$$

Case VIII

Neutral axis lies outside the section i.e. $0 \le k' \le 1$ and $1 \le k_t \le k_1$ (Fig. 7(b)).

The *M-P* interaction relation obtained for this case is:

$$\bar{M} = 3\alpha_1 \begin{bmatrix} \gamma\left(1+2r\right) + \alpha\beta\left(\alpha + 2r\right) - \frac{1}{3}\left(\frac{r}{k'}\right)^2 g_1^2 h_1 \\ + \frac{2S_L}{3}\left(\frac{r}{k'}\right)^2 \gamma a_1^2 f_L - \left(\psi + 2r\right)\beta_1 \bar{P} \end{bmatrix} \tag{37}$$

The non-dimensional distance of the neutral axis, *r*, required in the above equation and also for determining the value of k' from Eq. (7) may be obtained from the quadratic equation:

$$\left[-\frac{\left(1-k\right)^2}{2k} + \frac{S_L}{k}\gamma a_1^2\right] r^2 + \left[\alpha\beta + \gamma + \frac{1-k}{k} + \frac{2S_L}{k}\gamma a_1^2 - \beta_1 \bar{P}\right] r + \left[\alpha\beta + \gamma - \frac{1}{2k} + \frac{S_L}{k}\gamma a_1^2 - \beta_1 \bar{P}\right] = 0 \tag{38}$$

Case IX

Neutral axis lies outside the section i.e. $1 \le k\,' \le k_1$ and $1 \le k_t \le k_1$ (Fig. 7(c)).

The *M-P* interaction relation obtained for this case is:

$$\bar{M} = 3\alpha_1\left[\gamma(1+2r)+\alpha\beta(\alpha+2r)+\frac{2S_L}{3}\left(\frac{r}{k'}\right)^2\gamma a_1^2 f_L-(\psi+2r)\beta_1\bar{P}\right] \tag{39}$$

The non-dimensional distance of the neutral axis, *r*, required in the above equation and also for determining the value of k' from Eq. (7) may be obtained from the quadratic equation:

$$\left(\frac{S_L}{k}\gamma a_1^2\right)r+\left[\alpha\beta+\gamma+\frac{S_L}{k}\gamma a_1^2-\beta_1\bar{P}\right]=0 \tag{40}$$

Case X

Neutral axis lies outside the section i.e. $1 \le k\,' \le k_1$ and $k_1 \le k_t \le k_2$ (Fig. 7(d)).

The *M-P* interaction relation obtained for this case is:

$$\bar{M} = 3\alpha_1\left[\alpha\beta(\alpha+2r)+\gamma(1+2r)+\frac{2S_L}{3}\left(\frac{r}{k'}\right)^2\left(\gamma a_1^2 f_L+\beta b_1^2 g_L\right)-(\psi+2r)\beta_1\bar{P}\right] \tag{41}$$

where

$$f_1 = \alpha k - k_1 \tag{42}$$

The non-dimensional distance of the neutral axis, r, required in the above equation and also for determining the value of k' from Eq. (7) may be obtained from the quadratic equation:

$$\left[\frac{S_L}{k}a_1^2(\beta+\gamma)\right]r^2+\left[\alpha\beta+\gamma+2\frac{S_L}{k}\left(\gamma a_1^2+\beta a_1 f_1\right)-\beta_1\bar{P}\right]r+\left[\alpha\beta+\gamma+\frac{S_L}{k}\left\{\gamma a_1^2+\beta f_1^{\,2}\right\}-\beta_1\bar{P}\right]=0 \tag{43}$$

Case XI

Neutral axis lies outside the section i.e. $k_1 \le k\,' \le k_2$ and $k_1 \le k_t \le k_2$ (Fig. 7(e)).

The *M-P* interaction relation obtained for this case is:

$$\bar{M} = 3\alpha_1\left[\gamma(1+2r)+\alpha\beta(\alpha+2r)+\frac{2S_L}{3}\left(\frac{r}{k'}\right)^2\left(\gamma a_1^2 f_L+\beta b_1^2 g_L-c_1^2 h_L\right)-(\psi+2r)\beta_1\bar{P}\right] \tag{44}$$

The non-dimensional distance of the neutral axis, *r*, required in the above equation and also for determining the value of k' from Eq. (7) may be obtained from the linear equation:

$$\left[\gamma+\alpha\beta+\frac{2S_L}{k}\left(\gamma a_1^2+\beta a_1 f_1+a_1 k_1\right)-\beta_1\bar{P}\right]r+\left[\alpha\beta+\gamma+\frac{S_L}{k}\left(\gamma a_1^2+\beta f_1^{\,2}-k_1^2\right)-\beta_1\bar{P}\right]=0 \tag{45}$$

The *M-P* interaction curves of linear hardening model for the *T*-section taken earlier have been plotted in Fig. 8 by taking different values of *k*.

3.3.2 Parabolic-hardening

Eleven cases which depend upon the position of the neutral axis are required for the parabolic hardening model, which are discussed in this section.

Case I

Neutral axis lies in the web i.e. $k_1 \le k' \le k_2$ and $k_1 \le k_t \le k_2$ (Fig. 6(a)).

The *M-P* interaction relation obtained for this case is:

$$\bar{M} = 3\alpha_1 \begin{bmatrix} \alpha\beta(r-2\alpha) - \gamma\left(\frac{r}{k'}\right)^2\left(\frac{2}{3}-k^2\right) - (\psi-2r)\beta_1\bar{P} \\ +\gamma r^2 + \frac{S_P}{4}\left(\frac{r}{k'}\right)^2\left[\gamma a_1^2 f_P - \beta b_1^2 g_P + c_1^2 h_P\right] \end{bmatrix} \tag{46}$$

The non-dimensional distance of the neutral axis, *r*, required in the above equation and also for determining the value of k' from Eq. (5) may be obtained from the quadratic equation:

$$\gamma\left[2+\frac{S_P}{k}\left(a_1^2-d_1^2\right)\right]r^2 - \left[3\gamma+2\frac{S_P}{k}\left\{\gamma a_1^2+\beta d_1 e_1 - k_1 d_1\right\} - \alpha\beta - \beta_1\bar{P}\right]r + \left[\gamma+\frac{S_P}{k}\left\{\gamma a_1^2 - k_1^2 + \beta e_1^2\right\} - \alpha\beta - \beta_1\bar{P}\right] = 0 \tag{47}$$

where

$$S_P = \frac{2}{3(k_2-k_1)}\left(\frac{\sigma_{ud}}{\sigma_{yd}} - 1\right) \tag{48}$$

$$f_P = 5k + 3k_1 \tag{49a}$$

$$g_P = 5k_t + 3k_1 \tag{49b}$$

$$h_P = 5k' + 3k_1 \tag{49c}$$

Case II

Neutral axis lies in the web i.e. $k_1 \le k' \le k_2$ and $1 \le k_t \le k_1$ (Fig. 6(b)).

The *M-P* interaction relation obtained for this case is:

$$\bar{M} = 3\alpha_1 \begin{bmatrix} \alpha\beta(2r-\alpha) - \gamma\left(\frac{r}{k'}\right)^2\left(\frac{2}{3}-k^2\right) - (\psi-2r)\beta_1\bar{P} \\ +\gamma r^2 + \frac{S_P}{4}\left(\frac{r}{k'}\right)^2\left[\gamma a_1^2 f_P + c_1^2 h_P\right] \end{bmatrix} \tag{50}$$

The non-dimensional distance of the neutral axis, *r*, required in the above equation and also for determining the value of k' from Eq. (5) may be obtained from the quadratic equation:

$$\left[2\gamma+\frac{S_P}{k}\left(\gamma a_1^2 - d_1^2\right)\right]r^2 - \left[3\gamma - \alpha\beta + 2\frac{S_P}{k}\left\{\gamma a_1^2 - k_1 d_1\right\} - \beta_1\bar{P}\right]r + \left[\gamma - \alpha\beta + \frac{S_P}{k}\left\{\gamma a_1^2 - k_1^2\right\} - \beta_1\bar{P}\right] = 0 \tag{51}$$

Case III

Neutral axis lies in the web i.e. $1 \le k' \le k_1$ and $0 \le k_t \le 1$ (Fig. 6(c)).

The *M-P* interaction relation obtained for this case is:

$$\bar{M} = 3\alpha_1\left[\gamma r^2 + \alpha\beta(2r-\alpha) - \gamma\left(\frac{r}{k'}\right)^2\left(\frac{2}{3}-k^2\right) + \frac{S_P}{4}\left(\frac{r}{k'}\right)^2 \gamma a_1^2 f_P - (\psi - 2r)\beta_1\bar{P}\right] \tag{52}$$

The non-dimensional distance of the neutral axis, *r*, required in the above equation and also for determining the value of k' from Eq. (5) may be obtained from the quadratic equation:

$$\gamma\left(2+\frac{S_P}{k}a_1^2\right)r - \left[\gamma - \alpha\beta + \frac{S_P}{k}\gamma a_1^2 - \beta_1\bar{P}\right] = 0 \tag{53}$$

Case IV

Neutral axis lies in the web i.e. $1 \le k' \le k_1$ and $0 \le k_t \le 1$ (Fig. 6(d)).

The *M-P* interaction relation obtained for this case is:

$$\bar{M} = 3\alpha_1\left[\begin{array}{l} r^2 - \left(\frac{r}{k'}\right)^2\left\{\frac{1}{3}(1+\gamma) - \gamma k^2 + \frac{2}{3}\beta k_t^3\right\} \\ + \frac{S_P}{4}\left(\frac{r}{k'}\right)^2 \gamma a_1^2 f_P - (\psi - 2r)\beta_1\bar{P} \end{array}\right] \tag{54}$$

The non-dimensional distance of the neutral axis, *r*, required in the above equation and also for determining the value of k' from Eq. (5) may be obtained from the quadratic equation:

$$\left[1+\gamma+\frac{\beta}{2k}+\frac{\beta k}{2}+\frac{S_P}{k}\gamma a_1^2\right]r^2 - \left[1+2\gamma+\alpha\beta k+\frac{\beta}{k}+2\frac{S_P}{k}\gamma a_1^2 - \beta_1\bar{P}\right]r + \left[\gamma+\frac{1}{2}\alpha^2\beta k+\frac{\beta}{2k}+\frac{S_P}{k}\gamma a_1^2 - \beta_1\bar{P}\right] = 0 \tag{55}$$

Case V

Neutral axis lies in the flange i.e. $0 \le k' \le 1$ and $0 \le k_t \le 1$ (Fig. 6(e)).

The *M-P* interaction relation obtained for this case is:

$$\bar{M} = 3\alpha_1\left[\begin{array}{l} r^2 - \frac{1}{3}\left(\frac{r}{k'}\right)^2\left(1+2\gamma-\gamma k^2-2\beta k_t^3\right) \\ + \frac{S_P}{4}\left(\frac{r}{k'}\right)^2 \gamma a_1^2 f_P - (\psi - 2r)\beta_1\bar{P} \end{array}\right] \tag{56}$$

The non-dimensional distance of the neutral axis, *r*, required in the above equation and also for determining the value of k' from Eq. (5) may be obtained from the quadratic equation:

$$\left[1+\gamma+\frac{\beta}{2k}+\frac{\beta k}{2}+\frac{S_P}{k}\gamma a_1^2\right]r^2 - \left[1+2\gamma+\alpha\beta k+\frac{\beta}{k}+\frac{2S_P}{k}\gamma a_1^2 - \beta_1\bar{P}\right]r + \left[\gamma+\frac{\beta}{2k}+\frac{\alpha^2\beta k}{2}+\frac{S_P}{k}\gamma a_1^2 - \beta_1\bar{P}\right] = 0 \tag{57}$$

Case VI

Neutral axis lies in the flange i.e. $0 \le k' \le 1$ and $0 \le k_t \le 1$ (Fig. 6(f)).

The *M-P* interaction relation obtained for this case is:

$$\bar{M} = 3\alpha_1 \begin{bmatrix} \frac{1}{3}\left(\frac{r}{k'}\right)^2 \left\{\gamma k^2 - \gamma + 2\left(k'\right)^3 + 2\beta k_t^3\right\} \\ + \frac{S_P}{4}\left(\frac{r}{k'}\right)^2 \gamma a_1^2 f_P - \left(\psi - 2r\right)\beta_1 \bar{P} \end{bmatrix} \tag{58}$$

The non-dimensional distance of the neutral axis, *r*, required in the above equation and also for determining the value of k' from Eq. (5) may be obtained from the quadratic equation:

$$\left[\gamma\left(1-\frac{1}{2k}\right) - \frac{k}{2} + \frac{\beta k}{2} + \frac{S_P}{k}\gamma a_1^2\right] r^2 - \left[\alpha\beta k + \gamma\left(2-\frac{1}{k}\right) + \frac{2S_P}{k}\gamma a_1^2 - \beta_1 \bar{P}\right] r + \left[\frac{\alpha^2 \beta k}{2} + \gamma\left(1-\frac{1}{2k}\right) + \frac{S_P}{k}\gamma a_1^2 - \beta_1 \bar{P}\right] = 0 \tag{59}$$

Case VII

Neutral axis lies outside the section i.e. $0 \le k' \le 1$ and $0 \le k_t \le 1$ (Fig. 7(a)).

The *M-P* interaction relation obtained for this case is:

$$\bar{M} = 3\alpha_1 \begin{bmatrix} \gamma\left(1+2r\right) - \frac{1}{3}\left(\frac{r}{k'}\right)^2 \gamma g_1^2 h_1 - \frac{\alpha^2 \beta k}{3}\frac{\alpha + 3r}{1+r} \\ + \alpha\beta k_t \left(\alpha + 2r\right) + \frac{S_P}{4}\left(\frac{r}{k'}\right)^2 \gamma a_1^2 f_P - \left(\psi + 2r\right)\beta_1 \bar{P} \end{bmatrix} \tag{60}$$

The non-dimensional distance of the neutral axis, *r*, required in the above equation and also for determining the value of k' from Eq. (7) may be obtained from the quadratic equation:

$$\left[-\gamma\frac{\left(1-k\right)^2}{2k} + \frac{S_P}{k}\gamma a_1^2\right] r^2 + \left[\alpha\beta k + 2\gamma - \frac{\gamma}{k} - 2\frac{S_P}{k}\gamma a_1^2 - \beta_1 \bar{P}\right] r + \left[\frac{\alpha^2 \beta k}{2} + \gamma\left(1-\frac{1}{2k}\right) + \frac{S_P}{k}\gamma a_1^2 - \beta_1 \bar{P}\right] = 0 \tag{61}$$

Case VIII

Neutral axis lies outside the section i.e. $0 \le k' \le 1$ and $1 \le k_t \le k_1$ (Fig. 7(b)).

The *M-P* interaction relation obtained for this case is:

$$\bar{M} = 3\alpha_1 \begin{bmatrix} \gamma\left(1+2r\right) + \alpha\beta\left(\alpha + 2r\right) - \frac{1}{3}\left(\frac{r}{k'}\right)^2 g_1^2 h_1 \\ + \frac{S_P}{4}\left(\frac{r}{k'}\right)^2 \gamma a_1^2 f_P - \left(\psi + 2r\right)\beta_1 \bar{P} \end{bmatrix} \tag{62}$$

The non-dimensional distance of the neutral axis, *r*, required in the above equation and also for determining the value of k' from Eq. (7) may be obtained from the quadratic equation:

$$\left[-\frac{\left(1-k\right)^2}{2k} + \frac{S_P}{k}\gamma a_1^2\right] r^2 + \left[\alpha\beta + \gamma + \frac{1-k}{k} + \frac{2S_P}{k}\gamma a_1^2 - \beta_1 \bar{P}\right] r + \left[\alpha\beta + \gamma - \frac{1}{2k} + \frac{S_P}{k}\gamma a_1^2 - \beta_1 \bar{P}\right] = 0 \tag{63}$$

Case IX

Neutral axis lies outside the section i.e. $1 \le k' \le k_1$ and $1 \le k_t \le k_1$ (Fig. 7(c)).

The *M-P* interaction relation obtained for this case is:

$$\bar{M} = 3\alpha_1\left[\gamma(1+2r)+\alpha\beta(\alpha+2r)+\frac{S_P}{4}\left(\frac{r}{k'}\right)^2\gamma a_1^2 f_P-(\psi+2r)\beta_1\bar{P}\right] \tag{64}$$

The non-dimensional distance of the neutral axis, *r*, required in the above equation and also for determining the value of k' from Eq. (7) may be obtained from the quadratic equation:

$$\left(\frac{S_P}{k}\gamma a_1^2\right)r+\left[\alpha\beta+\gamma+\frac{S_P}{k}\gamma a_1^2-\beta_1\bar{P}\right]=0 \tag{65}$$

Case X

Neutral axis lies outside the section i.e. $1\le k'\le k_1$ and $k_1\le k_t\le k_2$ (Fig. 7(d)).

The *M-P* interaction relation obtained for this case is:

$$\bar{M} = 3\alpha_1\left[\alpha\beta(\alpha+2r)+\gamma(1+2r)+\frac{S_P}{4}\left(\frac{r}{k'}\right)^2\left(\gamma a_1^2 f_P+\beta b_1^2 g_P\right)-(\psi+2r)\beta_1\bar{P}\right] \tag{66}$$

The non-dimensional distance of the neutral axis, *r*, required in the above equation and also for determining the value of k' from Eq. (7) may be obtained from the quadratic equation:

$$\left(\frac{S_P}{k}a_1^2(\beta+\gamma)\right)r^2+\left[\alpha\beta+\gamma+2\frac{S_P}{k}\left(\gamma a_1^2+\beta a_1 f_1\right)-\beta_1\bar{P}\right]r+\left[\alpha\beta+\gamma+\frac{S_P}{k}\left\{\gamma a_1^2+\beta {f_1}^2\right\}-\beta_1\bar{P}\right]=0 \tag{67}$$

Case XI

Neutral axis lies outside the section i.e. $k_1\le k'\le k_2$ and $k_1\le k_t\le k_2$ (Fig. 7(e)).

The *M-P* interaction relation obtained for this case is:

$$\bar{M} = 3\alpha_1\left[\gamma(1+2r)+\alpha\beta(\alpha+2r)+\frac{S_P}{4}\left(\frac{r}{k'}\right)^2\left(\gamma a_1^2 f_P+\beta b_1^2 g_P-c_1^2 h_P\right)-(\psi+2r)\beta_1\bar{P}\right] \tag{68}$$

The non-dimensional distance of the neutral axis, *r*, required in the above equation and also for determining the value of k' from Eq. (7) may be obtained from the linear equation:

$$\left[\alpha\beta+\gamma+\frac{2S_P}{k}\left(\gamma a_1^2+\beta a_1 f_1+a_1 k_1\right)-\beta_1\bar{P}\right]r+\left[\alpha\beta+\gamma+\frac{S_P}{k}\left(\gamma a_1^2+\beta {f_1}^2-k_1^2\right)-\beta_1\bar{P}\right]=0 \tag{69}$$

The *M-P* interaction curves of parabolic hardening model for the T-section taken earlier have been plotted in Fig. 9 by taking different values of *k*.

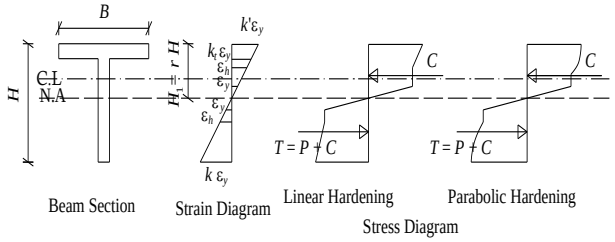

(a) Neutral axis lies in the web i.e. $k_1\le k'\le k_2$ and $k_1\le k_t\le k_2$.

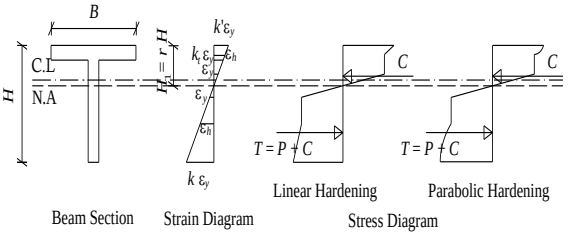

(b) Neutral axis lies in the web i.e. $k_1\le k'\le k_2$ and $1\le k_t\le k_1$.

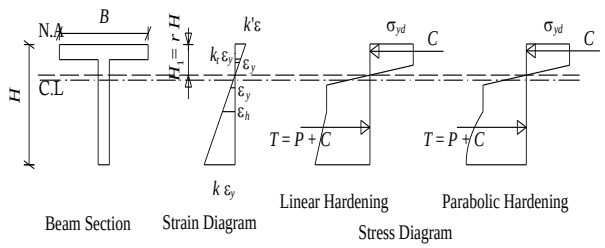

(c) Neutral axis lies in the web i.e. $1 \le k' \le k_1$ and $1 \le k_t \le k_1$.

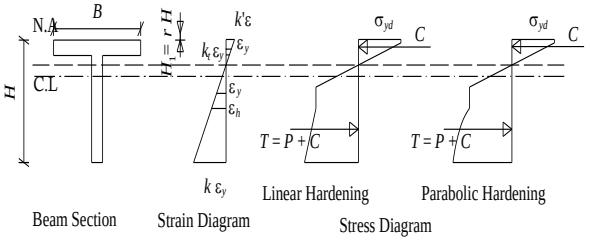

(d) Neutral axis lies in the web i.e. $1 \le k' \le k_1$ and $0 \le k_t \le 1$.

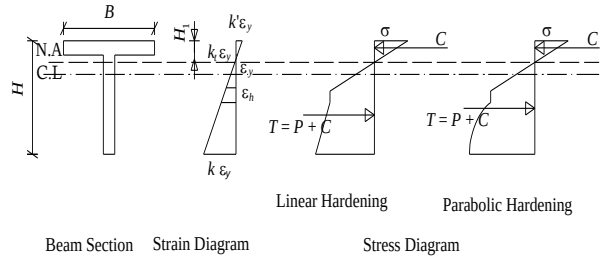

(e) Neutral axis lies in the web i.e. $0 \le k' \le 1$ and $0 \le k_t \le 1$.

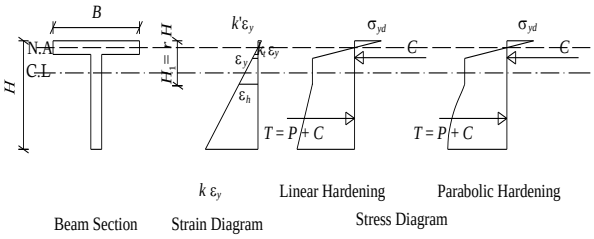

(f) Neutral axis lies in the flange i.e. $0 \le k' \le 1$ and $0 \le k_t \le 1$.

Fig.6
Stress and strain variation for positions of neutral axis inside the section for strain-hardening model.

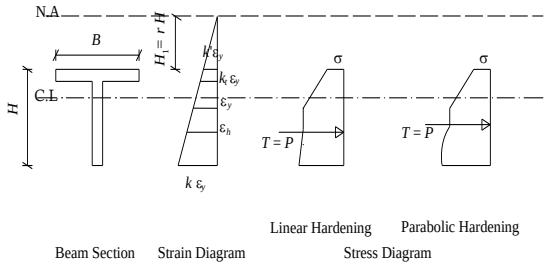

(a) Neutral axis lies outside the section i.e. $0 \le k' \le 1$ and $0 \le k_t \le 1$.

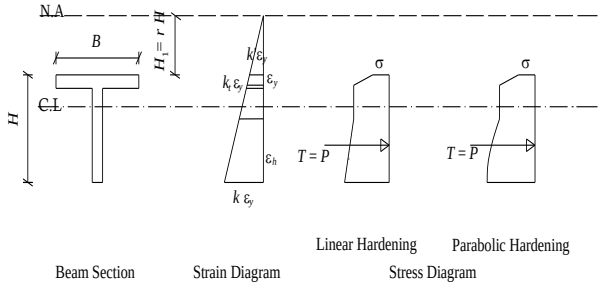

(b) Neutral axis lies outside the section i.e. $0 \le k' \le 1$ and $1 \le k_t \le k_1$.

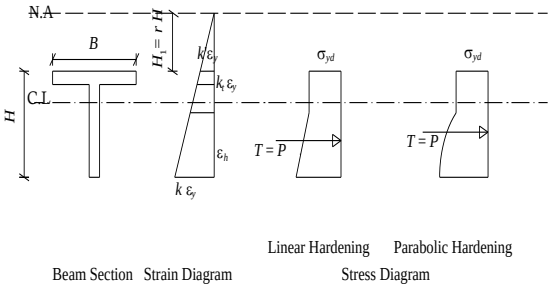

(c) Neutral axis lies outside the section i.e. $1 \le k' \le k_1$ and $1 \le k_t \le k_1$.

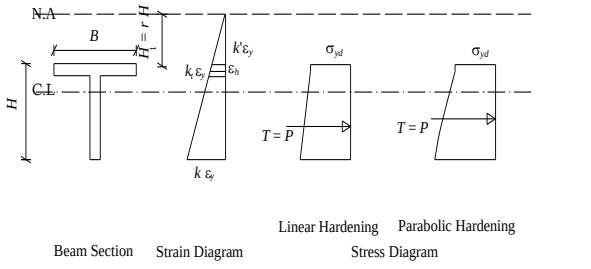

(d) Neutral axis lies outside the section i.e. $1 \le k' \le k_1$ and $k_1 \le k_t \le k_2$.

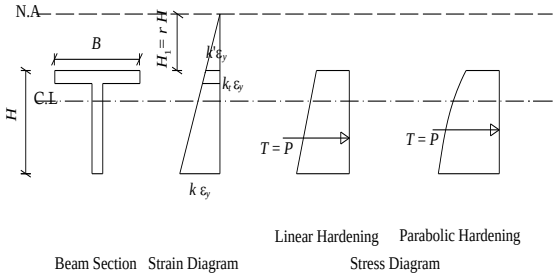

Fig.7
Stress and strain variation for positions of neutral axis outside the section for strain-hardening model.

(e) Neutral axis lies outside the section i.e. $k_1 \le k' \le k_2$ and $k_1 \le k_t \le k_2$.

3.4 Discussion

When there is no axial force, i.e. bending alone, the moment-curvature relations obtained from Eqs. (21), (22) and (46), (47) for the *T*-section considered earlier have been plotted in Fig. 10 for linear and parabolic hardening by taking the material characteristics from the tension test results of specimen 't036' . This curve has a strength stress endurance and linear curve has a weak status in stress curve. So the stress values of parabolic curve has a larger line in plastic.

The variable on the abscissa is the parameter, *k*, which is proportional to the curvature and is equal to the ratio of extreme fibre strain to the yield strain:

$$k = \frac{H}{2R\,\varepsilon_y} \tag{70}$$

where *R* is the radius of curvature. It is observed from this figure that there is little difference (~6%) between the predictions of the linear and parabolic hardening models for the particular material considered in Fig. 1. The moment-curvature relation for the linear hardening model is nearly linear, whereas, for parabolic hardening model there is a small curvature.

One quadrant of the *M-P* interaction curves for the *T*-section have been plotted already in Figs. 8 to 9 for linear and parabolic hardening models. The *M-P* interaction curves for all the models are plotted in Fig. 11. The observations made from these figures are:

a) Cases VIII and XI of the strain hardening models in Figs. 8 and 9 are required for a continuous curve, but from a practical perspective, the portion of the interaction curve represented by these cases is very small and could be ignored for linear as well as parabolic hardening materials. Therefore, only five cases: I, II, III, IV and V (first five for the neutral axis inside the section) are sufficient for practical purposes for defining the interaction curve of mild steel *T*-sections. All the five possible cases are required to define the interaction curve for an elastic-plastic material. The perfectly plastic has shown a smooth curve of strain increasing without increasing the stress. So the bold line curve in Fig. 8 has smaller p/p_y to M/M_y.
b) The strains and hence the strain rates due to bending and an axial force can be separated only for the linear-elastic case because the principle of superposition is not valid for the nonlinear case.(Fig 11)
c) The difference between the interaction curves for linear and parabolic hardening for the particular material illustrated in Fig. 1, is small (~6% when $\overline{P}$ is zero) which was evident from the small gap between the moment-curvature plots for the two cases.
d) The *M-P* interaction curves for elastic-plastic, as well as the strain hardening models, are non-convex for large values of the axial force when the neutral axis lies outside the section and are convex when the neutral axis lies inside the section.(Fig 11)

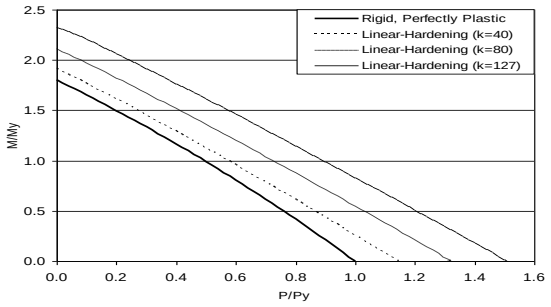

Fig.8
M-P interaction curves for linear hardening model for *T*-section ($T\ 100\ \times 100\ \times 10$).

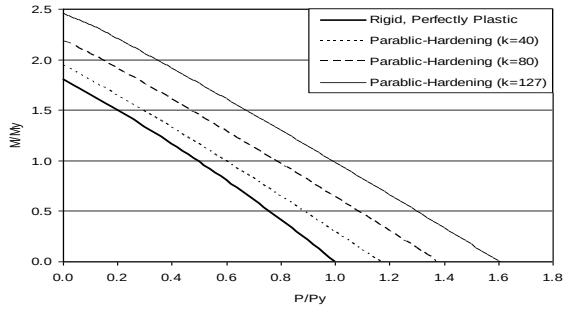

Fig.9
M-P interaction curves for parabolic hardening model for *T*-section ($T100\ \times 100\ \times 10$).

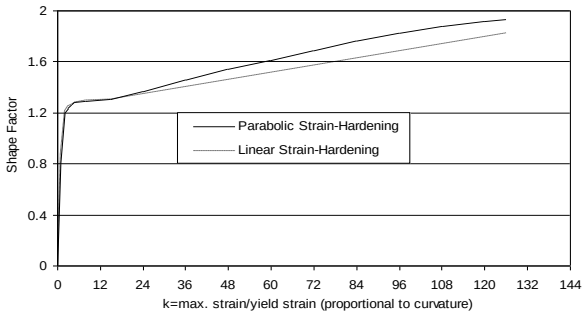

Fig.10
Moment-Curvature relation for different models.

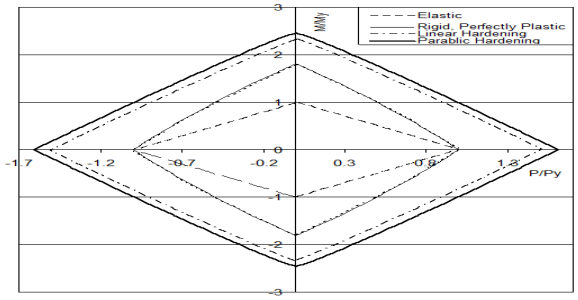

Fig.11
M-P interaction curves for different models ($k = k_1 = 127$ for linear and parabolic hardening curves) for *T*-section ($T100\ \times 100\ \times 10$).

4 CONCLUSIONS

The *M-P* (Bending Moment – Axial Force) interaction curves have been developed for *T*-section with linear and parabolic strain hardening idealisations of mild steel. The *M-P* interaction relations are expressed in terms of the extreme fibre strains, which is not possible for a rigid, perfectly plastic model. The relations are obtained for different practically possible cases related to different locations of neutral axis. These relations easily degenerate to rectangular section by some simple substitutions. The interaction curves of rectangular section can be obtained by some simple substitutions. One *T*-section, $T100\ \times 100\ \times 10$ was considered for studying the characteristics of interaction curves. The conclusions derived from this numerical study are:

(i) Although there are many possible cases related to different locations of neutral axis, but the portion of the interaction curve represented by many of these cases is very small and could be ignored for linear as well as parabolic hardening materials. It is found that only five cases, four for the neutral axis inside the section and one for the neutral axis outside the section (Cases IV, VIII and XI) are sufficient for practical purposes for defining the interaction curve of mild steel *T*-section.

(ii) The difference between the interaction curves for linear and parabolic hardening for the particular material is small (~6% when axial force is zero).

The *M-P* interaction curves for elastic-plastic, as well as the strain hardening models, are non-convex for large values of the axial force when the neutral axis lies outside the section and are convex when the neutral axis lies inside the section. Though the above conclusions are derived for the one typical *T*-section considered in the study but other *T*-sections being similar, the above conclusions may be considered to be general for any *T*-section.

APPENDIX A

Mathematical proofs

Linear hardening (CaseI)

The total compressive force on the section can be obtained by integrating the stress over the section in compression in Fig. 6(a), thus giving,

$$C=\sigma_{yd}\left[h\left(B-b\right)+bH_1\left(1-\frac{1}{2k'}\right)\right]+S_L\sigma_{yd}\left[BH_1\left(k'-k_1\right)\left(1-\frac{k_1}{k'}\right)-\left(B-b\right)\left(k_t-k_1\right)\left(H_1-h-\frac{k_1H_1}{k'}\right)\right] \tag{A.1}$$

or

$$C=P_{1yd}\left[\alpha\beta+\gamma r\left(1-\frac{1}{2k'}\right)+S_L\frac{r}{k'}\left\{\left(k'-k_1\right)^2-\beta\left(k_t-k_1\right)^2\right\}\right] \tag{A.2}$$

Similarly, the total tensile force in Fig. 6(a) is

$$T=\sigma_{yd}\left[b\left(H-H_1\right)-b\frac{H_1}{2k'}\right]+S_L\sigma_{yd}\left[b\left(k-k_1\right)\left(H-H_1-\frac{k_1}{k'}H_1\right)\right] \tag{A.3}$$

or

$$T=P_{1yd}\left[\gamma\left(1-r\right)-\gamma\frac{1-r}{2k}+S_L\frac{r}{k'}\gamma\left(k-k_1\right)^2\right] \tag{A.4}$$

The distance of the line action of the resultant compressive and tensile forces from the neutral axis can be found by taking the moment of the different force components, thus giving,

$$\begin{aligned}\bar{y}_C=&\frac{3M_{1yd}}{C}\left[\alpha\beta\left(r-2\alpha\right)+\gamma r^2\left\{-\frac{1}{3\left(k'\right)^2}\right\}\right]\\&+2S_L\frac{M_{1yd}}{C}\left(\frac{r}{k'}\right)^2\left[\left(k'-k_1\right)^2\left(2k'-k_1\right)-\beta\left(k_t-k_1\right)^2\left(2k_t-k_1\right)\right]\end{aligned} \tag{A.5}$$

and

$$\bar{y}_T=\frac{3M_{1yd}}{T}\left[\gamma\left(1-r\right)^2-\gamma\frac{\left(1-r\right)^2}{6k^2}\right]+2S_L\frac{M_{1yd}}{T}\left(\frac{r}{k'}\right)^2\left[\gamma\left(k-k_1\right)^2\left(2k+k_1\right)\right] \tag{A.6}$$

The position of the neutral axis can be found by considering the equilibrium of forces,

$$P = T - C \tag{A.7}$$

which using Eqs. (A.2) and (A.4) gives

$$P = P_{1yd}\left[\gamma(1-2r)-\alpha\beta+S_L\frac{r}{k'}\left\{\gamma\left(k-k'\right)^2-\left(k'-k_1\right)^2+\beta\left(k_t-k_1\right)^2\right\}\right] \tag{A.8}$$

from which the position of neutral axis is

$$\begin{aligned}&\gamma\left[2+\frac{S_L}{k}\left(a_1^2-d_1^2\right)\right]r^2-\left[3\gamma+2\frac{S_L}{k}\left\{\gamma a_1^2+\beta d_1 e_1-k_1 d_1\right\}-\alpha\beta-\beta_1\bar{P}\right]r\\&+\left[\gamma+\frac{S_L}{k}\left\{\gamma a_1^2-k_1^2+\beta e_1^2\right\}-\alpha\beta-\beta_1\bar{P}\right]=0\end{aligned} \tag{A.9}$$

which is same as Eq. (22) in this work. The moment of bending resistance of the section is

$$M = C\bar{y}_C + T\bar{y}_T - P\left(\frac{H}{2}\psi - H_1\right) \tag{A.10}$$

or,

$$\overline{M} = \frac{C\,\overline{y}_C}{M_{yd}} + \frac{T\,\overline{y}_T}{M_{yd}} - \frac{PH}{2M_{yd}}(\psi - 2r) \tag{A.11}$$

which substituting Eqs. (A.2) to (A.8), we get Eq. (21), i.e.

$$\bar{M} = 3\alpha_1\left[\begin{array}{l}\alpha\beta(r-2\alpha)-\gamma\left(\frac{r}{k'}\right)^2\left(\frac{2}{3}-k^2\right)-(\psi-2r)\beta_1\bar{P}\\+\gamma r^2+\frac{2S_L}{3}\left(\frac{r}{k'}\right)^2\left[\gamma a_1^2 f_L-\beta b_1^2 g_L+c_1^2 h_L\right]\end{array}\right] \tag{A.12}$$

REFERENCES

[1] Menkes S.B., Opat H.J., 1973, Broken beams, *Experimental Mechanics* **13**: 480-486.

[2] Jones N., 1976, Plastic failure of ductile beams loaded dynamically, *Journal of Engineering for Industry* **98**: 131-136.

[3] Liu J.H., Jones N., 1987, Experimental investigation of clamped beams struck transversely by a mass, *International Journal of Impact Engineering* **6**(4): 303-335.

[4] Liu J.H., Jones N., 1988, *Plastic Failure of a Clamped Beams Struck Transversely by a Mass*, University of Liverpool, Department of Mechanical Engineering Report ES/13/87.

[5] Jones N., Soares C.G., 1977, Higher model dynamic, plastic behavior of beam loaded impulsively, *International Journal of Mechanical Sciences* **20**: 135-147.

[6] Shen W.Q., Jones N. A., 1992, Failure criterion for beams under impulsive loading, *International Journal of Impact Engineering* **12**(1): 101-121.

[7] Alves M., Jones N., 2002, Impact failure of beams using damage mechanics: Part II – Application, *International Journal of Impact Engineering* **27**(8): 863-90.

[8] Symonds P.S., Genna F., Ciullini A., 1991, Special cases in study of anomalous dynamic elastic-plastic response of beams by a simple model, *International Journal of Solids and Structures* **27**(3): 299-314.

[9] Qian Y., Symonds P.S., 1996, Anomalous dynamic elastic-plastic response of a Galerkin beam model, *International Journal of Mechanical Sciences* **38**(7): 687-708.

[10] Bassi A., Genna F., Symonds P.S., 2003, Anomalous elastic-plastic responses to short pulse loading of circular plates, *International Journal of Impact Engineering* **28**(1): 65-91.

[11] Lellep J., Torn K., 2005, Shear and bending response of a rigid-plastic beam subjected to impulsive loading, *International Journal of Impact Engineering* **31**(9): 1081-1105.
[12] Ma G. W., Shi H. J., Shu D. W., 2007, P–I diagram method for combined failure modes of rigid-plastic beams, *International Journal of Impact Engineering* **34**(6): 1081-1094.
[13] Ghaderi S. H., Kazuyuki H., Masahiro F., 2009, Analysis of stationary deformation behavior of a semi-infinite rigid-perfect plastic beam subjected to moving distributed loads of finite width, *International Journal of Impact Engineering* **36**(1): 115-121.
[14] Li Q. M., Liu Y. M., 2003, Uncertain dynamic response of a deterministic elastic–plastic beam, *International Journal of Impact Engineering* **28**(6): 643-651.
[15] Li Q. M., Liu Y. M., Ma G. W., 2006, The anomalous region of elastic–plastic beam dynamics, *International Journal of Impact Engineering* **32**(9): 1357-1369.
[16] Xi F., Liu F., Li Q. M., 2012, Large deflection response of an elastic, perfectly plastic cantilever beam subjected to a step loading, *International Journal of Impact Engineering* **48**: 33-45.
[17] Brake M. R., 2012, An analytical elastic-perfectly plastic contact model, *International Journal of Solids and Structures* **49**(22): 3129-3141.
[18] Hosseini M., Abbas H., 2013, Strain hardening in M–P interaction for metallic beam of I-section, *Thin-Walled Structures* **62**: 243-256.
[19] Alves M., Jones N., 2002, Impact failure of beams using damage mechanics, Part I – Analytical model, *International Journal of Impact Engineering* **27**(8): 837-61.